Astroparticle Physics 70 (2015) 39–53

Contents lists available at ScienceDirect

Astroparticle Physics

journal homepage: www.elsevier.com/locate/astropart

Propagation in 3D spiral-arm cosmic-ray source distribution models and secondary particle production using Picard

R. Kissmann [a,*], M. Werner [a], O. Reimer [a], A.W. Strong [b]

[a] Institut für Astro- und Teilchenphysik, Leopold-Franzens-Universität Innsbruck, A-6020 Innsbruck, Austria
[b] Max Planck Institut für extraterrestrische Physik, Postfach 1312, D-85741 Garching, Germany

ARTICLE INFO

Article history:
Received 27 November 2014
Received in revised form 17 March 2015
Accepted 8 April 2015
Available online 17 April 2015

Keywords:
Cosmic rays: propagation
Methods: numerical
Diffusion

ABSTRACT

We study the impact of possible spiral-arm distributions of Galactic cosmic-ray sources on the flux of various cosmic-ray nuclei throughout our Galaxy. We investigate model cosmic-ray spectra at the nominal position of the sun and at different positions within the Galaxy. The modelling is performed using the recently introduced numerical cosmic ray propagation code Picard. Assuming non-axisymmetric cosmic-ray source distributions yields new insights on the behaviour of primary versus secondary nuclei.

We find that primary cosmic rays are more strongly confined to the vicinity of the sources, while the distribution of secondary cosmic rays is much more homogeneous compared to the primaries. This leads to stronger spatial variation in secondary to primary ratios when compared to axisymmetric source distribution models. A good fit to the cosmic-ray data at Earth can be accomplished in different spiral-arm models, although leading to decisively different spatial distributions of the cosmic-ray flux. These lead to different cosmic ray anisotropies, where even reproducing the data becomes possible. Consequently, we advocate directions to seek best fit propagation parameters that take into account the higher complexity introduced by the spiral-arm structure on the cosmic-ray distribution. We specifically investigate whether the flux at Earth is representative for a large fraction of the Galaxy. The variance among possible spiral-arm models allows us to quantify the spatial variation of the cosmic-ray flux within the Galaxy in presence of non-axisymmetric source distributions.

1. Introduction

The majority of Galactic cosmic-ray transport models assume our Galaxy to be azimuthally symmetric, thus allowing the solution of the transport problem efficiently in 2D cylindrical coordinates. The Milky Way, however, is known to be a spiral Galaxy (see, e.g., [47]). Apart from the imprint on the gas distribution and the magnetic field (see, e.g. [29,24]), the Galactic spiral arms are also thought to have an important impact on the distribution of the sources of Galactic cosmic rays (see, e.g. [37,22,15]). This idea is motivated by cosmic-ray source candidates like pulsars and supernova remnants being rather young (see, e.g. [36,54–56]) and therefore mostly confined to the vicinity of the star-formation regions and thus to the vicinity of the spiral arms. Just recently, supernova remnants (SNRs) have received observational support as sources of cosmic rays (see [2]), supporting the link between cosmic-ray sources candidates and star-forming regions.

Nevertheless, in most of the Galactic cosmic-ray propagation models the sources are explicitly assumed to be axisymmetrically distributed in the Galaxy (see, e.g. [41,3]). Currently, however, we witness a transition in Galactic cosmic-ray modelling from two-dimensional azimuthally symmetric models to those that allow higher degrees of realism. Recent studies of Galactic cosmic-ray propagation assuming a spiral-arm source distribution for the cosmic rays, e.g., include those by Benyamin et al. [15], Effenberger et al. [22], Gaggero et al. [25]; and Werner et al. [51].

Shaviv et al. [38] emphasized that an inhomogeneous source distribution should help to explain the observed increase in the positron fraction (see [5,9]). Correspondingly, Gaggero et al. [25] found that a spiral-arm source distribution can be used to explain the observed leptonic cosmic-ray spectra at Earth. For this reason, additional primary sources of positrons were introduced. Furthermore, Benyamin et al. [15] showed that the a spiral-arm source distribution can be used to explain the observed cosmic-ray Boron/Carbon ratio (B/C) in a plain-diffusion model by taking the relative motion between Earth and the spiral arms into account.

These studies used a particular realisation for the spiral-arm source distribution each, where significant differences occur

* Corresponding author.
E-mail address: ralf.kissmann@uibk.ac.at (R. Kissmann).

http://dx.doi.org/10.1016/j.astropartphys.2015.04.003
0927-6505/

between the different models (see, e.g., the different spiral-arm models used in [22,15]). These different choices reflect the different appearance of the Galactic spiral-arm structure in different tracers together with the problematic position of the observer within the Galaxy (see [40,47]).

This shows that, when exploring effects of a spiral-arm source distribution model, there is no unique such model. Properties of the spiral-arm model that differ between the various studies include the number of the spiral arms, their pitch-angle, their width, and their tangent longitudes. Consequently, Werner et al. [51] systematically investigated the impact of different such source distributions on the model cosmic-ray spectra and the corresponding spatial distribution of hadronic and leptonic cosmic rays.

Here, we expand the study by Werner et al. [51] by taking the effects of the nuclear reaction network into account. Apart from demonstrating a fit of the secondary-to-primary ratios at the location of the sun, as is done in the models discussed above, also an investigation of the spatial variation of these quantities is warranted (see, e.g. [37] for a discussion of the variation of ^{10}Be/^{9}Be). This relates to the question, whether the cosmic-ray fluxes observed at the location of the sun are representative for other regions in the Galaxy.

In the presence of spiral-arm cosmic-ray source distributions the role of the propagation parameters needs to be re-addressed: can the standard parameters (see, e.g. [45]) be adapted to allow a similarly good fit to the data in the presence of a spiral-arm source distribution, and what consequences arise for discrepancies? This also relates to the question of whether there are constraints from the cosmic-ray data that can be used to isolate a single model from the multitude of possible spiral-arm model realisations. A problematic constraint is the observed cosmic ray anisotropy in the 1 TeV range, where propagation models using an axisymmetric source distribution often predict a dipole amplitude of the anisotropy about an order of magnitude higher than is observed (see [23,44]).

We will address these points as follows. First we will briefly introduce the numerical framework used for the solution of the Galactic cosmic-ray propagation problem, where the validity of the scheme is demonstrated in the appendix. Then we discuss our specific simulation setup in conjunction with the considered spiral-arm models. Subsequently, we present the results from different spiral-arm source distribution models. Finally, we will conclude with a discussion of the consequences, where we demonstrate that the transition from axisymmetric to spatially three-dimensional modelling, including azimuthal variation, will allow to put further constraints on the cosmic-ray transport models, especially when combined with an analysis of the diffuse Galactic gamma-ray emission.

2. Numerical solution

In this study we numerically compute the cosmic-ray flux in the Galaxy using the recently introduced code Picard. This code solves the cosmic-ray transport equation on a numerical grid with three spatial and one momentum dimension (for details, see [31]). There, it was shown that Picard is particularly efficient in computing high resolution steady state solutions of the transport equation.

With regard to the implementation of the nuclear reaction network, which is essential to the present study, there are some important differences to other widely-used propagation codes like, e.g., galprop (for the discussion of the nuclear network in the context of galprop see e.g., [42,43]). Like in galprop the transport equation is first solved for the heaviest nucleus ${}^{N}_{Z}$X in the nuclear reaction network. From the resulting distribution function the contribution of nucleus ${}^{N}_{Z}$X to the secondary spallation source term of all lighter particles can be computed. Subsequently the transport equation is solved for the isotope ${}^{N-1}_{Z}$X, where the solution proceeds to the element having charge $Z-1$ when all isotopes of the element with charge Z have been addressed.

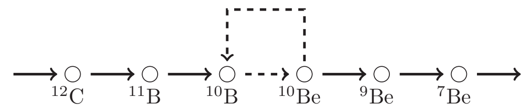

Fig. 1. Illustration of our handling of the nuclear network. In Picard the transport equation is only solved repeatedly in the range of the nuclear network, where a later (to the right in the image) nucleus can decay into an earlier one (to the left in the image). For more details see the text.

In this way all nuclei are ordered so that most of them only decay (via spallation or radioactive decay) into nuclei which occur later in the network (for an illustration see Fig. 1). There are, however, a few nuclei that potentially produce secondaries that have already been treated earlier in the nuclear reaction network. Therefore, repeated runs of the entire network with a typical number of two network iterations (see e.g., [42]) are required in galprop.

We use a different strategy in Picard, where only parts of the network subject to the above effect are repeated. For this we first identify those nuclei that can decay into nuclei that appear earlier in the ordering scheme described above. Then only those parts of the network affected by this decay need to be solved repeatedly (for the specific example of the decay ^{10}Be $\rightarrow$ ^{10}B see Fig. 1, where the local network iteration is illustrated by the dashed arrows). This is much more efficient than a repetition of the entire network, thus allowing several repetitions of the potentially affected parts of the network with the same computational effort. galprop uses the same time-integration scheme to obtain a solution for each network iteration, thus, leading to the same numerical cost for the computation of each network iteration. In contrast, the solver used in the Picard code detects whether a solution has been found, thus, allowing to compute a solution to the transport equation more quickly in repeated solutions for the same particle. In total the different implementation of the solution strategy of the nuclear reaction network results in a much higher efficiency in case of Picard, which also allows using a significantly higher number of network iterations. As discussed in Appendix A.3.2, in most cases two network iterations are sufficient to lead to a accurate solution for all relevant species. We will describe the specific setup that is used in the following.

3. Propagation models setups

Apart from the capability to efficiently handle spatially 3D transport problems, the new solver introduced in the Picard code offers the convenient feature to use the same transport parameters as the widely used galprop code (see http://sourceforge.net/projects/galprop/); we use the same implementation of the nuclear cross-sections (see, e.g., [42]) and of the various energy-loss processes (see, e.g. [41]).

This allows us to use well-established propagation parameters sets. Furthermore, this enables us to adopt parameters addressed in 2D model setups to initialize 3D model realisations. In Appendix A we document the validity of this approach quantitatively.

In this study we use the 2D reference models ${}^{S}Y^{Z}4^{R}20^{T}150^{C}5$, ${}^{S}Y^{Z}4^{R}30^{T}150^{C}5$, ${}^{S}Y^{Z}8^{R}20^{T}150^{C}5$, and ${}^{S}Y^{Z}8^{R}30^{T}150^{C}5$ from Ackermann et al. [4], which will be referred to as models z4R20, z4R30, z8R20 and z8R30[1], respectively. This set of propagation

[1] Model z8R20 is only used in the investigation of the numerical setup in Appendix A, where it was found to be not suitable for a 3D simulation setup.